AAPS PharmSciTech, Vol. 15, No. 2, April 2014 (© 2014)
DOI: 10.1208/s12249-014-0080-4

Research Article

Mixed Polyethylene Glycol-Modified Breviscapine-Loaded Solid Lipid Nanoparticles for Improved Brain Bioavailability: Preparation, Characterization, and *In Vivo* Cerebral Microdialysis Evaluation in Adult Sprague Dawley Rats

Zhidong Liu,[1,2,4] Chukwunweike Ikechukwu Okeke,[1,2] Li Zhang,[1,2] Hainan Zhao,[1,2] Jiawei Li,[1,2,3] Mike Okweesi Aggrey,[1,2] Nan Li,[1,2] Xiujun Guo,[1,2] Xiaochen Pang,[1,2] Lili Fan,[1,2] and Lili Guo[1,2]

Received 25 September 2013; accepted 7 January 2014; published online 31 January 2014

Abstract. Breviscapine is used in the treatment of ischemic cerebrovascular diseases, but it has a low bioavailability in the brain due to its poor physicochemical properties and the activity of P-glycoprotein efflux pumps located at the blood–brain barrier. In the present study, breviscapine-loaded solid lipid nanoparticles (SLN) coated with polyethylene glycol (PEG) derivatives were formulated and evaluated for their ability to enhance brain bioavailability. The SLNs were either coated with polyethylene glycol (40) (PEG-40) stearate alone (Bre-GBSLN-PS) or a mixture of PEG-40 stearate and 1,2-distearoyl-*sn*-glycero-3-phosphoethanolamine-N-PEG2000 (DSPE-PEG_{2000}) (Bre-GBSLN-PS-DSPE) and were characterized both *in vitro* and *in vivo*. The mean particle size, polydispersity index, and entrapment efficiency for Bre-GBSLN-PS and Bre-GBSLN-PS-DSPE were 21.60±0.10 and 22.60±0.70 nm, 0.27±0.01 and 0.26 ±0.04, and 46.89±0.73% and 47.62±1.86%, respectively. The brain pharmacokinetic parameters revealed that the brain bioavailability of breviscapine from the Bre-GBSLN-PS and Bre-GBSLN-PS-DSPE was significantly enhanced ($p<0.01$) with the area under concentration–time curve (AUC) of 1.59±0.39 and 1.42±0.58 μg h/mL of breviscapine, respectively, in comparison to 0.11±0.02 μg h/mL from the commercial breviscapine injection. The ratios of the brain AUC for scutellarin in comparison with the plasma scutellarin AUC for commercial breviscapine injection, Bre-GBSLN-PS, and Bre-GBSLN-PS-DSPE were 0.66%, 2.82%, and 4.51%, respectively. These results showed that though both SLN formulations increased brain uptake of breviscapine, Bre-GBSLN-PS-DSPE which was coated with a binary combination of PEG-40 stearate and DSPE-PEG_{2000} had a better brain bioavailability than Bre-GBSLN-PS. Thus, the coating of SLNs with the appropriate PEG derivative combination could improve brain bioavailability of breviscapine and can be a promising tool for brain drug delivery.

KEY WORDS: breviscapine; microdialysis; mixed PEGylation; P-glycoprotein (P-gp); solid lipid nanoparticles.

INTRODUCTION

Breviscapine is a traditional herbal drug extracted from the Chinese herb *Erigeron breviscapus* (Vant.) Hand.-Mazz. and contains two main flavonoids. The primary active component of breviscapine is scutellarin (4′,5,6-tetrahydroxyflavone-7-*O*-glucuronide) which makes up more than 90% of the extract and the second component apigenin-7-*O*-glucuronide is only about 4% of the extract (1). Breviscapine has several commercially produced preparations like tablets and injections available in the market and has been widely used in the clinic to treat acute cerebral infarction and paralysis induced by cerebrovascular diseases such as hypertension, cerebral thrombosis, and cerebral hemorrhage (2,3). However, like lots of other naturally extracted flavonoid drugs with proved pharmacological activities, the clinical application of breviscapine has been limited due to its poor physicochemical properties such as low aqueous solubility and poor chemical stability which results to a limited bioavailability with an absolute bioavailability of only 0.40± 0.19% reported for oral preparations (4,5). Adding to the poor physicochemical properties of breviscapine is the daunting challenge posed by the blood–brain barrier (BBB) in delivering the drug molecules into the brain. The BBB is a very restrictive anatomical and dynamic barrier that regulates the traffic of molecules into and out of the brain environment through an

Zhidong Liu and Chukwunweike Ikechukwu Okeke contributed equally to this work.

[1] Tianjin State Key Laboratory of Modern Chinese Medicine, Tianjin University of Traditional Chinese Medicine, 88 Yuquan Road, Tianjin, 300193, People's Republic of China.
[2] Engineering Research Center of Modern Chinese Medicine Discovery and Preparation Technique, Ministry of Education, Tianjin University of Traditional Chinese Medicine, 88 Yuquan Road, Tianjin, 300193, People's Republic of China.
[3] Department of Experimental Education, Tianjin University of Traditional Chinese Medicine, Tianjin, 300193, People's Republic of China.
[4] To whom correspondence should be addressed. (e-mail: lonerliuzd@163.com)

array of mechanisms that include, but not limited to, enzymatic activities and active efflux of molecules by the endogenous efflux transport systems such as the P-glycoprotein (P-gp) located at the cerebrovascular endothelial cell membranes (6,7). P-gp is a multidrug resistance protein that is expressed in many organs and tissues including the BBB (8). Thus, P-gp could be involved in the elimination of breviscapine from the brain extracellular fluid (ECF).

Attempts have been made to develop novel delivery systems to either improve the physicochemical properties or increase the brain bioavailability of breviscapine. Polymeric nanoparticles (9), liposomes (5), and nanosuspension (10) formulations of breviscapine have been reported with some successes. However, these reports have various limitations such as effects of the reticuloendothelial system (RES), possible toxicity in the case of degradation of polymeric materials, and less objective methods of *in vivo* evaluation which involved evaluation of brain tissues post-sacrifice of the animals. Thus, to overcome these limitations, solid lipid nanoparticles (SLNs) would be a good useful alternative drug delivery carrier for breviscapine. SLNs have the advantage of using biocompatible and biodegradable biomaterials that could be engineered into suitable drug delivery carriers to improve the physicochemical properties of the drug molecules and enhance their ability to penetrate the BBB (11,12).

Surface modifications of solid lipid nanoparticles using polyethylene glycol (PEG) derivatives have also been reported to reduce uptake by the RES, with increased half-life in the circulation which would achieve either a passive or an active targeting of drugs to the brain (13). Previous researches had shown that a few common, nontoxic, and generally recognized as safe PEG derivatives that are used in drug formulations have an inhibitory effect on P-gp efflux pump, which are very much actively involved in restricting the penetration of drugs into the brain (14,15). Evaluation of brain drug concentrations in living and freely moving animals by *in vivo* cerebral microdialysis (MD) has also been shown to be an objective method of accessing the ECF concentration of drugs that cross the BBB (16). In this study, breviscapine SLNs coated with polyethylene glycol (40) (PEG-40) stearate were formulated and characterized, and its pharmacokinetic behavior in rat brain was compared with commercial breviscapine injection by *in vivo* microdialysis. We also tested the hypothesis that PEG-40 stearate coating could nonspecifically inhibit the P-gp efflux system and increase the brain uptake of breviscapine by doing an *in vitro* P-gp ATPase assay. A mixed modified formulation with a combination of PEG derivatives used as surface coating to the optimized formulation was also evaluated to determine if there is any added improvement in using a mixed PEG derivative coating in SLN drug delivery to the brain.

MATERIALS AND METHODS

Materials

Breviscapine (purity>90%) was purchased from Nanjing Zelang Medical Technology Co., Ltd., scutellarin (purity>98%) was purchased from Best Biotech Incorporation (Tianjin, China), 4 mg/mL commercial breviscapine injection was purchased from Jilin Longtai Pharmaceutical Company Ltd., (Jilin, China), *glyceryl behenate* (Compritol 888 ATO) was purchased from Gattefosse (France), palmitic acid was purchased from Sigma-Aldrich (USA), glyceryl monostearate (GMS), glyceryl tristearate (GTS), and stearic acid were obtained from Tianjin Guangfu Fine Chemical Research Institute (Tianjin, China), *PEG-40 stearate* (molecular weight (*Mw*)=*2,000 Da*) was purchased from Liaonang Aoke Nanotechnology Company (Liaoning, China), 1,2-distearoyl-*sn*-glycero-3-phosphoethanolamine-N-PEG2000 (DSPE-PEG_{2000}, Mw=2,000 Da) was acquired from Lipoid (Germany), MD34 dialysis bag (molecular weight cutoff (MWCO)=8,000–14,000 Da) was obtained from Solarbio® Life Sciences (Beijing, China), and Pgp-Glo™ assay kit was purchased from Promega (Promega Corporation, Madison, USA). All other chemicals used were of analytical grade and solvents were of high-performance liquid chromatography (HPLC) grade.

Lipid Screening by Differential Scanning Calorimetry (DSC)

DSC was used to select a suitable lipid core by estimating the solubility of breviscapine in various lipids as reported previously (17). Briefly, breviscapine/lipid solid dispersions were prepared by dissolving the drug in various melted lipids in a drug/lipid ratio of 1:10. The DSC thermal analysis of the solid dispersions was done to estimate drug solubility in lipid. The presence or absence of the drug characteristic peaks was used to select suitable lipids for the preparation of solid lipid nanoparticles. The thermal study was done using a PerkinElmer Jade DSC (PerkinElmer Analytical Instruments, Shanghai Co. Ltd) and result was analyzed with Pyris software. Samples (5–10 mg) were placed in a conventional aluminum pan and heated under nitrogen gas (20 mL/min) from 30°C to 220°C. Heating curves were recorded at a scan speed of 10°C/min.

Preparation of Breviscapine SLNs

SLNs were prepared from warm oil in water (o/w) microemulsion precursors as previously described (18) with some modifications. Briefly, specified amounts of lipids (glyceryl monostearate for Bre-GMSLN-PS or glyceryl behenate for Bre-GBSLN-PS formulations), Solutol®HS15, and PEG-40 stearate (PS) were weighed into glass vials and heated to 75°C. Breviscapine (10 mg) was dissolved in 3 mL of ethanol and dispersed in aliquots into the melted lipid and surfactant mixture. The mixture was stirred at 500 rpm and ethanol was completely removed under reduced pressure. Using a separate glass vial, deionized water (10 mL) was preheated to 75°C and added into the oil phase in aliquots. The spontaneously formed microemulsion was stirred for 30 min at 75°C. By cooling of the warm microemulsion to room temperature, the SLNs were then solidified. For Bre-GBSLN-PS-DSPE formulation, 1 mL of a 20-mg/mL DSPE-PEG_{2000} solution was added 10 min before cooling.

Each solid lipid nanoparticle formulation was filter sterilized and ultra-centrifuged at 4,000 rpm for 30 min in a centrifuge tube fitted with a filter membrane (MWCO=10,000), to separate the unencapsulated breviscapine and unattached surfactants.

Measurement of Size and Zeta Potential of SLNs

The mean particle size and polydispersity index of the SLN formulations were determined by photon correlation spectroscopy using Zetasizer Nano-ZS (Malvern Instruments, Malvern, UK). Each sample was diluted to a suitable concentration (1:25) with a 0.22-μm filtered micropore deionized water. Analysis was performed at 25°C using an angle of detection of 133°. The zeta potential of dispersions was also determined using Zetasizer Nano-ZS (Malvern Instruments, Malvern, UK). The samples were diluted suitably with deionized water. Particle size and charge on SLN were determined in triplicate and recorded as their mean values ± SD.

Entrapment Efficiency and Drug Loading

Entrapment efficiency (EE %) and drug loading (DL %) were determined by ultrafiltration–centrifugation technique (19). To determine the concentration of free drug (unentrapped) in the aqueous medium, 0.3 mL of breviscapine-loaded SLNs diluted with 3.2 mL deionized water was placed in the upper chamber of a centrifuge tube fitted with an ultrafilter (Amiconultra, Millipore Co., USA, MWCO 10 kDa) and centrifuged for 30 min at 4,000×*g*. The total content of drug in the aqueous medium was determined by dissolving 0.3 mL of the breviscapine-loaded SLN suspension with absolute ethanol. The resulting free and total drug samples were diluted appropriately using methanol and analyzed with the validated HPLC method described in the "Breviscapine Assay" section below. The EE was calculated as follows:

$$\mathrm{EE}(\%) = \frac{M_{\text{Total drug}} - M_{\text{Free drug}}}{M_{\text{Total drug}}} \times 100 \quad (1)$$

And drug loading was calculated as follows:

$$\mathrm{DL}(\%) = \frac{M_{\text{Total drug}} - M_{\text{Free drug}}}{M_{\text{Total lipid}} + \left(M_{\text{Total drug}} - M_{\text{Free drug}}\right)} \times 100 \quad (2)$$

where $M_{\text{Total drug}}$ was mass of total drug content, $M_{\text{Free drug}}$ was mass of free unentrapped drug, and $M_{\text{Total lipid}}$ was mass of total lipid added in system.

Transmission Electron Microscopy (TEM)

The TEM of the nanoparticles was done to observe the morphology of the nanoparticles. The SLNs were diluted in deionized water and a drop was placed on a copper grid to form a thin film of the suspension. The film was allowed to air dry and was negatively stained with 2% phosphotungstic acid. The samples were examined using a JEOL 100-II transmission electron microscope (JEOL, Tokyo, Japan).

Powder X-ray Diffractometry (PXRD)

The PXRD pattern of breviscapine, lyophilized blank SLNs, physical mixture of drug with lyophilized blank SLNs, and lyophilized drug-loaded SLNs was obtained using an X-ray diffractometer (Rigaku D/max 2500v/pc, Tokyo, Japan) fitted with a PW R18 X-ray generator. Nickel-filtered Cu Kα1 radiation having a wavelength of 1.54056 Å, operating at 40 kW and 200 mA, was used. All samples were run at 1° $(2\theta)\,\mathrm{min}^{-1}$ from 3° to 60°.

In Vitro Drug Release Study in PBS (pH 5.8)

In vitro breviscapine release studies were done by the dialysis method using phosphate-buffered saline (PBS) (pH 5.8) as the release medium. Before the release studies, the solubility of breviscapine in the release medium was measured. Briefly, excess amounts of breviscapine were dissolved in the medium in glass vials ($n=3$) and placed in a magnetic stirring water bath at a temperature of 37°C for a total of 70 h. At the end of test period, aliquots of samples were filtered, diluted appropriately, and assayed by a validated HPLC method to determine their concentrations. For release studies, 0.5 mL of breviscapine-loaded SLN suspensions or commercial breviscapine injection was pipetted into dialysis membrane bags (Solarbio® Life Sciences MWCO=8,000–14,000 Da) previously soaked in deionized water for 12 h. The bags were sealed and placed in 250 mL of PBS stirred at 50 rpm and maintained at 37°C using a drug dissolution tester (ZRS-8G, Tianjin, China). At predetermined times, 5.0-mL aliquots were taken from outside of the dialysis membrane and replaced with 5.0 mL of fresh media to maintain an equilibrium sink condition. Scutellarin concentration in each collected sample was measured by the validated HPLC method described in the "Breviscapine Assay" section below. Also, the particle sizes of SLNs inside the dialysis membranes were measured at the end of the release studies. Each sample was determined in triplicate.

Physical Stability of SLNs in Biologically Relevant Media at 37°C

To evaluate the stability of the breviscapine-loaded nanoparticles in biological relevant media, the SLNs were incubated at 37°C in deionized water and PBS (pH 5.8) for 12 h. The SLNs were diluted 1:10 *v/v* with the media and stirred at 50 rpm during the experiment duration. At predetermined time intervals, 1-mL aliquots were removed and allowed to equilibrate to room temperature prior to particle size measurements. The stability of the SLNs was assessed based on the retention of particle size.

Determination of Fixed Aqueous Layer Thickness (FALT), Incorporated Ratio of PEG (IR), and Average PEG Surface Density (SD_{PEG})

The FALT was determined using the Gouy–Chapman theory (20). According to this theory, the zeta potentials $\psi(L)$, described as the electrostatic potentials at the position of the slipping plane L (in nanometer), which is thought to occur just outside the fixed aqueous layer of the nanoparticle is expressed as:

$$\ln \psi(L) = \ln A - \kappa L \quad (3)$$

where A is regarded as a constant and κ is the Debye–Hückel parameter, that is equal to $\sqrt{C}/0.3$, and C is the molarity of electrolytes for a univalent salt. If zeta potentials are measured in various concentrations of NaCl and plotted against κ, the slope L gives the position of the slipping plane or thickness of the fixed aqueous layer in nanometer units. Based on this theory, the zeta potentials were measured in 0, 5, 10, 15, 50, and 100 mM NaCl solution and plotted against κ. FALT of PEG chains on the surface of Bre-GBSLN-PS and Bre-GBSLN-PS-DSPE was estimated from the slope of the plot in nanometer.

To determine the amounts of PEG attached on the surface of the nanoparticles (W_{PEG}), the PEG chains which were not incorporated into the nanoparticle membranes were separated by ultrafiltration in a centrifuge tube fitted with a MWCO 50-kDa ultrafilter (Amiconultra, Millipore Co., USA,). The PEG content in the filtrate (W_1) and total amount of PEG in unfiltered samples (W_2) were measured by a colorimetric method as previously reported (21). Briefly, 125 μL of an I_2/KI solution was added to 5 mL of a 1:100 diluted solution of the filtered or unfiltered samples. The reaction between the PEG and iodine was allowed to stand for 15 min in order for the color to develop. The PEG content was determined after a spectrophotometric measurement of the absorbance at 500 nm using a UV-2800H spectrophotometer (UNICO, China). The test samples were measured against a blank sample containing water and reagents only. A standard calibration curve was also established by taking the absorbance of known concentrations of PEG solution (2–30 μg/mL) and was used to the determine amount of PEG in samples. The incorporated ratio of PEG (IR) and SD_{PEG} were calculated using the formulas below:

$$W_{PEG} = W_2 - W_1 \tag{4}$$

Thus, the PEG IR was calculated as:

$$IR = W_{PEG}/W_2 \times 100\ \% \tag{5}$$

Calculations for the SD_{PEG} were done as follows:

The SD_{PEG} on the nanoparticles was estimated as the ratio of the total number of PEG molecules (N_{PEG}) to the total nanoparticle surface area (S_n),

$$\text{i.e.,}\quad SD_{PEG} = N_{PEG}/S_n \tag{6}$$

Solving for N_{PEG} and S_n,

$$N_{PEG} = (W_{PEG}/MW_{PEG}) \times A_n \tag{7}$$

where MW_{PEG} is molecular weight of PEG and A_n is Avogadro's number, and S_n=surface area of a sphere×total number of nanoparticles (N_p) in a volume unit.

Using $N_p = 6m/\pi r^3\rho$ and surface area of sphere$=4\pi r^2$,

$$S_n = 4\pi r^2 \times 6m/\pi r^3\rho \tag{8}$$

where m is mass of a volume unit of nanoparticles, ρ is density of nanoparticles (in grams per cubic centimeter) estimated to be 1.039 g/cm^3 from nanoparticle materials, and r (in nanometer) is approximated as radius of nanoparticles as measured by photon correlation spectroscopy.

Substituting for S_n and N_{PEG} in Eq. 6 above and simplifying, we obtain:

$$SD_{PEG} = W_{PEG}\cdot A_n\cdot r\cdot\rho\cdot 10^{-21}/3\cdot MW_{PEG}\cdot m \tag{9}$$

where 10^{-21} is the unit conversion factor.

Assessment of P-Glycoprotein ATPase Activity

The P-gp assay was designed to assess the contribution of active transport processes mediated by the P-gp to the brain pharmacokinetics especially uptake and elimination of breviscapine. P-gp ATPase assay is widely used to study susceptibility of drugs to P-gp efflux systems *in vitro* (22), and for this study, human P-pg membranes were used. Recombinant human P-gp membranes (Pgp-Glo™ Assay Systems) were purchased from Promega (Promega Corporation, Madison, USA), and the effects of the drug and the surfactants on P-gp ATPase activity were estimated by measuring the light generated from the ATP-dependent light-generating reaction of firefly luciferase. The inhibitory or stimulatory effect of breviscapine and the surfactants tested was examined against verapamil-stimulated P-gp ATPase activity. The method used was according to the manufacturer's protocol. Briefly, 20 μL of Pgp-Glo™ assay buffer, 20 μL of a 0.25 mM sodium orthovanadate (used as a selective inhibitor of P-gp ATPase), 20 μL of 0.5 mM verapamil (served as a positive control), 20 μL of breviscapine and surfactants in various concentrations, and 20 μL of a 1.25-mg/mL recombinant human P-gp membranes were added in turns into designated white opaque 96-well plate (Corning, USA) and incubated at 37°C for 5 min. The reaction was started by adding 10 μL of a 25 mM MgATP into all well except for the ATP standard-designated wells. Then, the plates were incubated at 37°C for 40 min. Subsequently, the plates were removed from the 37°C heat source, reactions stopped, and luminescence initiated by adding 50 μL of ATP detection reagent to all wells. Luminescent signal was allowed to develop at room temperature for 20 min, and then, the plate was read on a luminometer (flex station microplate reader). The changes in relative light units (ΔRLU) were determined by comparing sodium orthovanadate-treated samples with test samples and verapamil-treated samples, and thereafter, the test sample-stimulated P-gp ATPase activity was measured by converting the amount of ATP consumed with the aid of a standard calibration curve obtained using ATP standards.

Pharmacokinetics in Plasma

Adult male Sprague Dawley rats were provided by the Chinese Academy of Medical Sciences of Radiation Research Institute for the animal experiments. Ethical approval was obtained from the Animal Ethical Committee of the Tianjin University of Traditional Chinese Medicine for the animal studies (TCM-LAEC2013004). The care and use of the animals was conducted in accordance with the provisions of Laboratory Animal Administration ordinance issued by the

State Science and Technology Committee of the People's Republic of China (PR China), Act 2, and Laboratory Animal Administration regulations issued by the Tianjin Laboratory Animal Administration Office Tianjin, PR China. For the plasma pharmacokinetic study, the rats (250–290 g) were fasted overnight (12–16 h) prior to the study, but had access to drinking water *ad libitum.* The rats were divided into three groups of six each and each group received intravenous administration of 8 mg/kg breviscapine equivalent of either injection breviscapine, Bre-GBSLN-PS, or Bre-GBSLN-PS-DSPE through the lateral tail vein. Blood samples were collected from the retro-orbital vein of each rat into heparinized polypropylene microcentrifuge tubes at predetermined time intervals up to 12 h. The plasma was quickly separated by centrifugation at 4,000×*g* for 10 min and stored at −20°C until analysis. A validated method using ultra performance liquid chromatography fitted with tunable ultraviolet absorbance detection (UPLC-TUV) as described in the "Breviscapine Assay" section below was used for the determination of scutellarin concentration in plasma.

Pharmacokinetics in Brain

Stereotaxic Surgery

Adult male Sprague Dawley rats (220–260 g) were used for the *in vivo* brain microdialysis study. Before the surgery, the rats were anesthetized using 20% urethane (1,500 mg/kg IP). The surgical site was cleaned with iodine solution and the hair was shaved to expose the skin. The head of the rat was constrained on a rodent stereotaxic frame (Leica Angle Two™, USA). A midline anterior–posterior incision was made on the animal's scalp from the lambda to just in between the eyes. The exposed skull surface was dried using sterile swaps. An intracerebral guide cannula (Microbiotech/se AB, Stockholm, Sweden) was stereotaxically implanted into the cerebral cortex using the following stereotaxic coordinates: AP, −4.52; ML, 4.06 from bregma; and DV, −3.44 from the dura. The guide cannula was fixed with dental acrylic (Shanghai New Century Dental Material Co., Ltd.) which was also used to seal the exposed skull area. The guide cannula was plugged with a stainless steel temporary inner cannula and the animal allowed time to recover from the anesthesia before the brain MD experiment.

In Vivo Brain Microdialysis

In vivo MD was performed using Microbiotech/se AB microdialysis probes (Microbiotech/se AB, Stockholm, Sweden) with a polyethersulfone membrane length of 2 mm and molecular cutoff of 15 kDa. The MD probes were perfused with the perfusion solutions using a CMA 402 dual syringe pump fitted with 2.5 mL micro syringes (CMA/Microdialysis AB, Sweden). In MD studies, the *in vitro* or *in vivo* recovery is usually determined by the zero-net flux method (23) or by retrodialysis method (24). Since steady state would be difficult to reach in both plasma and ECF in a bolus injection experiment, the retrodialysis-by-drug method was used to estimate the *in vitro* and *in vivo* recovery for each probe used. For the *in vitro* recovery, the perfusate was a 5.0 μM scutellarin solution in artificial cerebrospinal fluid (aCSF) [NaCl 1.45 M, KCl 27 mM, $CaCl_2$ 12 mM, $MgCl_2$ 10 mM, Na_2HPO_4 20 mM, and EDTA-2Na 0.125% *w/v*], and a stirred 10-mL aCSF fluid maintained at 37°C was the *in vitro* ECF outside the probes. The probes were allowed to equilibrate for 30 min at a perfusion rate of 1.5 μL/min, after which single dialysate samples were collected over 30 min into mini-vials. Scutellarin concentration was measured in the outflow dialysate (C_{out}) and the inflow perfusate (C_{in}) and the recovery was calculated using Eq. 10 below:

$$\text{Recovery} = C_{in} - C_{out}/C_{in} \tag{10}$$

The MD probes were then inserted through the implanted intracerebral guide cannula into the predetermined position in the rat cerebral cortex and *in vivo* retrodialysis performed. For the *in vivo* recovery, the perfusate containing 20 μM of scutellarin in aCSF was perfused through the probes at 0.5 μL/min flow rate for at least 30 min to equilibrate. After the equilibration period, single dialysate samples were collected over 40 min and the concentrations were measured and *in vivo* recovery calculated using Eq. 10 above.

After the retrodialysis, each MD probe was equilibrated with drug-free aCSF at a flow rate of 0.5 μL/min for at least 1 h to wash out any drug left in the MD probe and tubing line. The rats were then successively administered intravenous bolus injection of the reference sample (breviscapine injection) and test samples (Bre-GBSLN-PS and Bre-GBSLN-PS-DSPE) at a dose volume equivalent to 8 mg/kg of breviscapine *via* the lateral tail vein. Microdialysate samples were collected at predetermined intervals for up to 12 h duration and were then analyzed using the validated HPLC-MS/MS analysis method described in the "Breviscapine Assay" section. A washout period of at least 10 h was allowed between successive administration of the breviscapine injection and the test sample solutions (Bre-GBSLN-PS and Bre-GBSLN-PS-DSPE) to each rat. The brain pharmacokinetics was calculated based on a non-compartmental model. Linear trapezoid method was used to estimate the area under the concentration–time curve (AUC) for each sample injected into each individual animal. All parameters were presented as mean ± SD.

Breviscapine Assay

Microdialysis Samples

The scutellarin concentrations in microdialysate samples were analyzed by a validated HPLC-MS/MS method. Microdialysate samples were not filtered or extracted. The chromatography was performed on a Shimadzu LC-20 System (Shimadzu Corporation, Japan) fitted with two Shimadzu LC-20AD pumps, SIL-20AC autosampler, and CTO-20A thermostat and controlled using CBM-20A controller. The chromatographic separation of scutellarin in injected samples (10 μL) was performed on an Agilent Zorbax XDB-C18 column (2.1× 50 mm, 3.5 μm, Agilent Technologies, USA) with gradient flow at 0.5 mL/min. The mobile phase was a blend of 0.1% formic acid in water (A) and 0.1% formic acid in methanol (B) and the gradient profile was 0 to 0.6 min, 2% (*v/v*) B; 0.6 to 0.9 min, linear gradient to 85% (*v/v*); 0.9 to 2.5 min, 85% (*v/v*) B; 2.5 to 2.51 min, linear gradient to 98% (*v/v*) B; 2.51 to

3.5 min, 98% (*v/v*); 3.5 to 3.51 min linear gradient to 2% (*v/v*); and 3.51 to 5.0 min, 2% (*v/v*) B.

The mass spectrometry was done on an API 4000 Qtrap® (AB SCIEX, USA) fitted with an ion spray source for electrospray ionization operating in a positive mode. Optimal instrument conditions (curtain gas, 15 psi; ion spray voltage, 5,000 V; temperature, 550°C; ion source gas 1, 60 psi; and ion source gas 2, 55 psi) were used to increase sensitivity and detection was by selected reaction monitoring of the strongest intensity product ion. Analyst® Software version 1.5.2 was used for instrument control and data analysis. The lower limit of quantification was 0.5 ng/mL and linear range was from 0.5 to 1,000 ng/mL.

Plasma Samples

The UPLC-TUV system used to analyze scutellarin in plasma samples consisted of a Waters Acquity UPLC® (Waters Corporation, USA) fitted with a Quaternary Solvent Manager, an Acquity UPLC® BEH C18 column (2.1× 50 mm, 1.7 μm) maintained at 30°C, a sample manager with a flow through needle, and a tunable ultraviolet absorbance detector set to 335 nm. Data were recorded and analyzed using the Empower® 3 chromatography data software. The mobile phase consisted of acetonitrile and acidified water (adjusted to pH 2.2 using phosphoric acid) at a ratio of 17:83 (*v/v*). The elution of scutellarin was achieved with an isocratic flow at a rate of 0.3 mL/min. Plasma samples collected were prepared before liquid chromatographic analysis (25). Drug extraction and protein precipitation of the samples were done by mixing 100 μL of plasma sample, 20 μL of internal standard working solution of baicalin (5 μg/mL), 1.0 mL of ethyl acetate, and 25 μL of 50% phosphoric acid, which was vortex mixed for 10 min followed by centrifugation at 3,000×*g* for 10 min. The supernatants were then transferred into another tube and evaporated to dryness. The residue was dissolved with 100 μL of the mobile phase and vortexed for 10 min. A 5-μL aliquot of the solution was injected into the UPLC-TUV for detection and quantification. A calibration curve used for the determination of scutellarin in plasma samples was obtained after analyzing various concentrations of a working solution of scutellarin and a constant concentration of the internal standard in rat plasma. An acceptable linearity was obtained for scutellarin in the concentration range of 0.05–100.00 μg/mL (R^2=0.999) after plotting the calibration curve with the ratios of the peak areas of scutellarin to the internal standard as the independent variable. The relative response factor was derived from the slope of the curve and used in determining the concentration of scutellarin in the collected plasma samples.

Physicochemical Evaluation Samples

All other samples from breviscapine-loaded SLN characterization were filtered and assayed with a reverse phase HPLC method consisting of an Agilent 1200 series (Agilent Technologies, Germany) equipped with an Agilent G1311A Quat pump and an Agilent G1315D diode array detector. The wavelength was set to 335 nm and the HPLC system was controlled by using the ChemStation software. The analytical column was a reverse phase Diamonsil® C18 (2) column (200×4.6 mm, 5 μm, Dikma Technologies Inc., USA) maintained at 30°C in a column oven and protected by a guard column (10×4.6 mm, Dikma Technologies Inc., USA). The mobile phase consisted of 76% acidified water (adjusted to pH 2.2 using phosphoric acid) and 24% acetonitrile. Elution of scutellarin was achieved with an isocratic flow at 1.0 mL/min. All samples were analyzed in triplicate.

Statistical Analysis

The non-compartmental pharmacokinetic parameters were calculated for each individual set of data obtained per experimental animal. All data reported are expressed as the mean ± SD. Statistical analyses were performed using the statistical analysis Student's *t* test with Microsoft excel.

RESULTS AND DISCUSSIONS

Preparation and Physicochemical Characterization of Breviscapine Solid Lipid Nanoparticles

The drug loading capacity of SLNs mainly depends on the solubility behavior of the drug in the lipid melt during and after formulation of the SLNs (26). So, in order to obtain sufficient drug loading and stable incorporation of breviscapine into the SLN lipid matrix, lipid solubility test for breviscapine in various lipids was performed by evaluating the DSC thermograms of breviscapine/lipid solid dispersions. As shown in Fig. 1, breviscapine showed an exothermic peak at 181°C. This peak was still present in the solid dispersions with stearic acid and glyceryl tristearate but disappeared in palmitic acid, glyceryl monostearate, and glyceryl behenate. Glyceryl monostearate and glyceryl behenate were selected for the preliminary SLN formulation and characterization. Although there were no breviscapine characteristic exothermic peaks in the thermogram for breviscapine/palmitic acid solid dispersion, palmitic acid could not be used for the SLN formulation. This was because it failed to yield a stable nanoparticle formulation in the one-factor experiments for all conditions tested and flocculated within 1 h. Similar observation was reported by Li *et al.* (27) where the drug solubility of tetrandrine was high in palmitic acid, but the formulation was unstable.

In the preliminary study, the concentrations of surfactant and co-surfactant, drug load, and experimental conditions such as stirring speed were varied in order to achieve a stable SLN formulation with glyceryl monostearate and glyceryl behenate as the lipid core (data not shown). In order to yield successful SLN formation, at least 1% (*w/v*) and 4% (*w/v*) of the surfactant (Solutol HS15) were required for Bre-GMSLN-PS and Bre-GBSLN-PS formulations, respectively. The co-surfactant and surface modifier, PEG-40 stearate, was added at 0.5% (*w/v*) to all formulations and the ratio of PEG-40 stearate to DSPE-PEG_{2000} in the Bre-GBSLN-PS-DSPE formulation was 5:2. The use of warm o/w microemulsion precursor method adapted for the formulation was simple and reproducible as previously reported (18).

The particle size, polydispersity index (PdI), and zeta potential of the formulated SLNs are shown in Table I. The formation and particle size of SLNs showed to be dependent on the amount of the surfactant used in the formulation, with higher concentrations leading to narrower particle size. At the

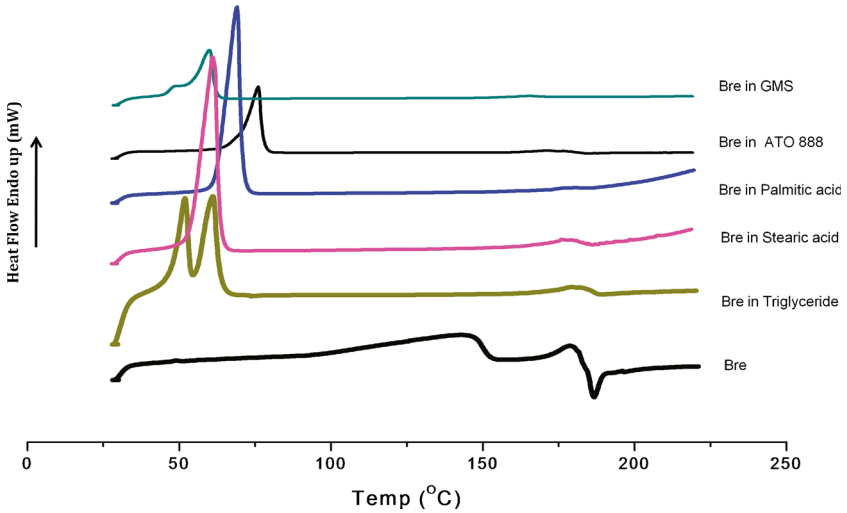

Fig. 1. Differential scanning calorimetry thermograms of breviscapine in different lipids

optimized surfactant concentrations as shown in Table I, the particle sizes were below 50 nm for Bre-GMSLN-PS, Bre-GBSLN-PS, and Bre-GBSLN-PS-DSPE. The Bre-GBSLN-PS-DSPE which was mixed modified with a stearate and DSPE-anchored PEG (molar weight 2,000) did show a similar particle size as the Bre-GBSLN-PS which was single modified with only the stearate-anchored PEG-40 (molar weight = 2,000). The PEG chains of these nanoparticles could act as a tighter mesh on the outside of these nano-vesicles, thus limiting the increase of particle size. According to a previous report, nanoparticles with particle size less than 80 nm have more penetrating ability across the BBB either *via* fluid endocytosis or phagocytosis (28). In addition, the PEG chains on nanoparticle surfaces are hydrophilic thereby preventing their interactions with blood proteins (opsonins) and reduces subsequent opsonization and phagocytosis by the RES (21).

PdI values for all formulations were less than 0.30 indicating relatively less poly-dispersed SLN suspensions, and the zeta potential ranged from −5 to −13.2 mV. High static potential (>30 mV) on the surface of nanoparticles is widely accepted to lead to a more stable nanoparticle. However, this does not strictly apply to formulations which contain steric stabilizers such as PEG side chains, which decreases the zeta potential due to a shift in the shear plane of the particle (29).

The entrapment efficiency of all the SLN formulations as determined by the ultrafiltration–centrifugation technique was in the range of 37–47% with drug loading ranging from 3.66% to about 6% (Table I). A marginal improvement in the entrapment efficiency of Bre-GBSLN-PS and Bre-GBSLN-PS-DSPE over Bre-GMSLN-PS could be due to the favored partitioning of breviscapine into the glyceryl behenate lipid matrix. A hundred percent entrapment efficiency is rarely observed in lipophilic drug delivery. Other factors apart from the solubility of drug in lipid that can limit entrapment efficiency include the chemical and physical structure of solid lipid matrix as well as polymorphic state of lipid material in nanoparticles. (29,30).

TEM

The TEM images in Fig. 2 showed that the shape of the SLNs was almost spherical. Also, the size of the SLNs determined by the photon correlation spectroscopy was consistent with the TEM results. The diameters determined by TEM were 34.1±6.3, 29.9±2.2, and 29.1±1.6 nm for Bre-GMSLN-PS, Bre-GBSLN-PS, and Bre-GBSLN-DSPE, respectively; while using the photon correlation spectroscopy, the sizes were 29.9±5.2, 21.6±0.1, and 22.6±0.7 nm, respectively.

PXRD

The breviscapine-powdered X-ray diffractogram showed numerous sharp peaks at 2θ of 10.1, 14.4, 16.1, 19.2, 20.3, 21.1, 24.3, 25.9, 29.0, 30.4, 31.5, and 44.3 (Fig. 3) which suggests the crystalline nature of the drug. The PXRD for the blank GBSLN-PS showed broad peaks at 2θ of 19.1 and 23.2 and the diffraction patterns of the drug-loaded GBSLN formulations were comparable to the blank GBSLN-PS. By using the peak intensity to estimate the degree of crystallinity of drug in SLNs, the reduction or absence of typical breviscapine peaks in drug-loaded SLN formulations confirms the partial or complete loss of crystallinity of the drug in lipid matrix. The Bre-GMSLN-PS PXRD pattern showed a partial reduction in the intensity of the drug peak at 2θ of 21.1, and this suggests the drug is not completely converted to its amorphous state in the Bre-GMSLN-PS, whereas for the Bre-GBSLN-PS and Bre-GBSLN-PS-DSPE formulations, the intense drug peaks were not present suggesting a complete conversion of drug to its amorphous state in the GBSLNs.

In Vitro Drug Release Study in PBS (pH 5.8)

In vitro release of breviscapine injection and SLN formulations is shown in Fig. 4. Breviscapine has been reported to have aqueous solubility of 14–60 μg/mL (10,31). So, to maintain sink conditions, PBS at pH 5.8 was used as the release medium for the *in vitro* release studies of the breviscapine formulations. The solubility of breviscapine in PBS 5.8 at 37°C was determined to be 740.0±18.0 μg/mL (n=3) as measured by HPLC. Thus, for the release studies, 0.5 mL of breviscapine SLNs or breviscapine injection containing 1,000 μg/mL of breviscapine was pipetted into a dialysis

Table I. Compositions of Breviscapine Solid Lipid Nanoparticles and Their Physicochemical Properties

Composition (mg/mL)						
Formulations	Breviscapine	Glyceryl monostearate	Glyceryl behenate	Solutol HS 15	PEG-40 stearate	DSPE-PEG
Bre-GMSLN-PS	1.0	10.0	–	20	5.0	–
Bre-GBSLN-PS	1.0	–	7.0	60	5.0	–
Bre-GBSLN-PS-DSPE	1.0	–	7.0	60	5.0	2.0
Summary of physicochemical properties						
Formulations	Particle size (nm)	PdI	Zeta potential (mV)	Entrapment Efficiency (%)	Drug loading (%)	Drug released in 2 h (%)
Bre-GMSLN-PS	29.9±5.2	0.20±0.08	−13.2±3.9	37.96±0.18	3.66±0.02	50.59±7.61
Bre-GBSLN-PS	21.6±0.1	0.27±0.05	−5.8±1.0	46.89±0.73	6.28±0.09	36.20±2.68
Bre-GBSLN-PS-DSPE	22.6±0.7	0.26±0.04	−7.2±1.4	47.62±1.86	6.37±0.23	39.02±1.49

Each data point is mean ± SD (n=3)
PdI polydispersity index

membrane bag and immersed into 250 mL of the release medium. Breviscapine injection showed a rapid drug release indicating permeability of the membrane to the drug. The release profiles of all SLN formulations exhibited an initial burst effect, and the percentage of drug content released from Bre-GMSLN-PS, Bre-GBSLN-PS, and Bre-GBSLN-PS-DSPE was about 50%, 36%, and 39%, respectively, after 2 h (Table I). However, the Bre-GBSLNs showed a much relatively lower burst release than the Bre-GMSLN-PS, and this could be due to a better drug partitioning in the glyceryl behenate lipid matrix as confirmed in the PXRD studies. This suggests that encapsulation of breviscapine in GBSLNs coated with PEG-40 stearate alone or in combination with DSPE-PEG_{2000} changed the drug release behavior, and subsequently, the SLNs would affect its biodistribution *in vivo* compared with free breviscapine solution. Also, the particle sizes of the Bre-GMSLN-PS changed significantly after 12 h (data not shown) which indicates loss of stability of the nanoparticle formulation in the dissolution medium used.

Physical Stability of SLNs in Biologically Relevant Media at 37°C

The physical stability of breviscapine nanoparticles was evaluated by monitoring changes of particle sizes at 37°C in deionized water and PBS 5.8 which were used to simulate physiological conditions. As shown in Fig. 5, the particle sizes of Bre-GBSLN-PS and Bre-GBSLN-PS-DSPE slightly increased after the 12-h incubation period but remained below 50 nm. This was not the case with the Bre-GMSLN-PS as there was a significant increase in particle size in both deionized water (p<0.05) and PBS 5.8 (p<0.001). A similar result has been previously reported when glyceryl monostearate was used as the lipid matrix in SLN formulation (32,33). This loss of stability by Bre-GMSLN during incubation in physiological medium could be due to the high percentage of monoglycerides in glyceryl monostearate which increases its hydrophilicity and emulsifying property, hence reducing lipid stability in the medium.

P-Glycoprotein ATPase Activity

The P-gp ATPase activity study helped to ascertain the susceptibility of breviscapine to the P-gp efflux pump and the potential for the PEG-coated SLN formulation to inhibit P-gp efflux pumps and improve the penetration of breviscapine across the BBB. The effective inhibition of the P-gp efflux pumps is being considered as a potential strategy to improve the brain bioavailability of CNS-active drugs. Previous studies have showed that certain chemical components including PEG derivatives, used as surfactants or surface-coating materials, have the tendency to inhibit P-gp efflux pumps through several mechanisms (14,34,35). Figure 6 shows the P-gp ATPase activity of breviscapine and the different surfactants used in the SLN formulations as compared with the basal- and verapamil-stimulated P-gp ATPase activity. The ATPase activities of

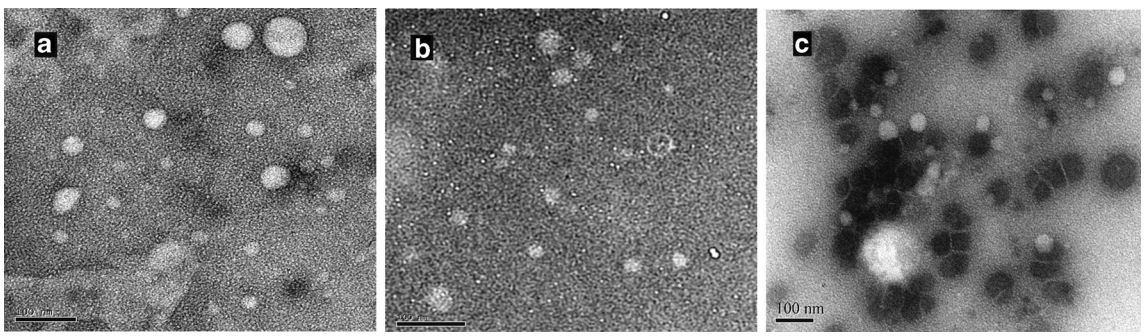

Fig. 2. Transmission electron micrograph of solid lipid nanoparticles. **a** Bre-GMSLN-PS, **b** Bre-GBSLN-PS, **c** Bre-GBSLN-PS-DSPE

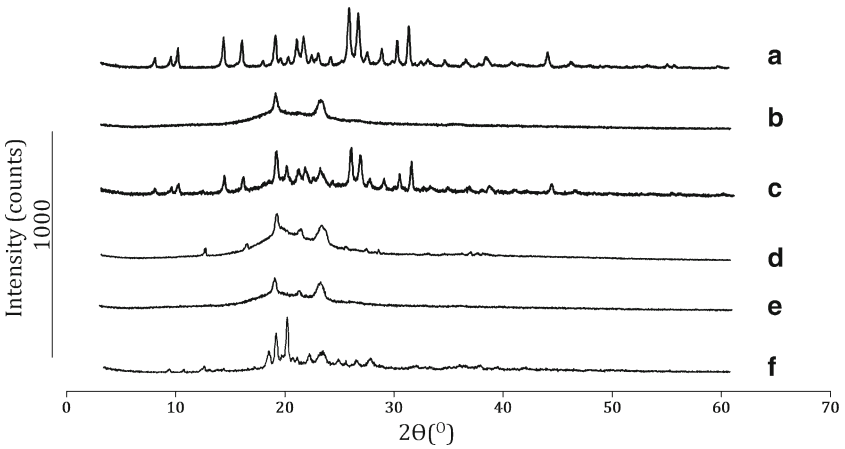

Fig. 3. XRD diffractogram for *a* Breviscapine, *b* freeze-dried blank nanoparticles, *c* physical mixture of freeze-dried blank nanoparticles and Breviscapine (3:5), *d* freeze-dried Bre-GBSLN-PS, *e* freeze-dried Bre-GBSLN-PS-DSPE, and *f* freeze-dried Bre-GMSLN-PS

breviscapine and verapamil were 2-fold higher than that of basal ATPase activity which indicates that breviscapine is a substrate for the P-gp efflux pumps. Among the surfactants tested, DSPE-PEG_{2000} solution showed a decrease in ATPase activity, and Solutol HS15 and PEG-40 stearate had a 1.5-fold and 2.6-fold increase, respectively, in ATPase activity at the concentrations tested. In a previous study to determine the P-gp ATPase activity of PEG-40 stearate, it was reported that PEG-40 stearate could competitively inhibit the activity of P-gp efflux pumps by saturating the P-gp receptors as a substrate and, as a result, decrease its efflux activity (15). DSPE-PEG has also been shown to be an allosteric inhibitor of P-gp, which reduces both verapamil-induced and basal ATPase activity (35). Though the exact mechanism(s) of P-gp inhibition by PEG derivatives is yet to be fully elucidated, our observations from the P-gp ATPase activity assay were in agreement with these previous reports. Consequently, the use of PEG derivatives in surface modification of SLNs could result to increased drug uptake across membranes that would otherwise restrict drug transport due to overexpression of P-gp efflux pumps. More so, a binary mixture of these PEG derivatives could have some synergistic inhibitory activity through various mechanisms. However, there is need for more definitive studies of the mechanism of P-gp inhibition by PEG derivatives and indeed other multidrug-resistant reversing surfactants.

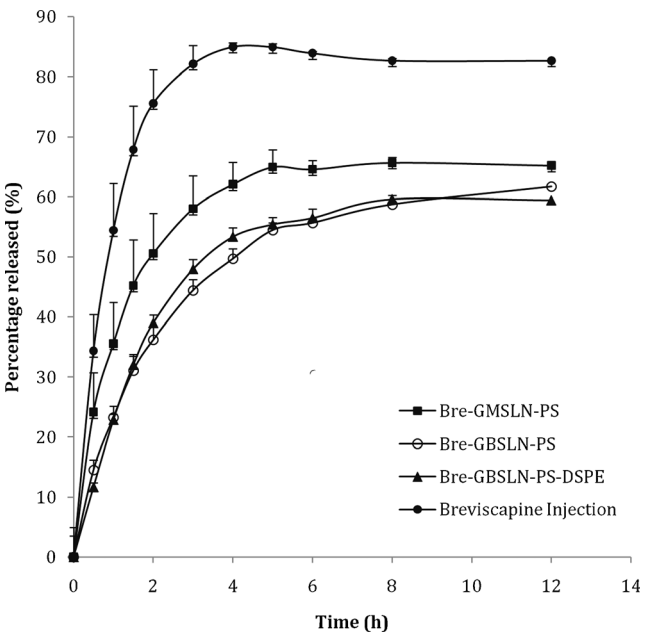

Fig. 4. *In vitro* release profile of breviscapine in PBS (pH 5.8). Each *data point* represents mean value, *error bars* represent SD (n=3)

FALT, Incorporated Ratio of PEG (IR), and SD_{PEG}

Bre-GBSLN-PS and Bre-GBSLN-PS-DSPE formulations were chosen for the surface modification studies of the breviscapine nanoparticles. As shown in Table II, the grafting of the DSPE-anchored PEG onto the PEG-40 stearate-modified Bre-GBSLN-PS (at a PEG-40 stearate/DSPE-PEG_{2000} ratio of 5:2) did not result to any significant increase in the FALT (p>0.05), instead there was a small decrease in FALT for the mixed modified formulation. Similar observation was made in the PEG surface densities (SD_{PEG}) for both formulations. These results were in good agreement with previous reports about mixed PEG-modified nano-vesicles. In a study involving the PEG coating of nanoparticles with PEG of varied chain lengths, Cauda *et al.* reported that the surface density depends on PEG chain length (36). In their study, the samples coated with PEG550, PEG5000, and a mixture of PEG550–PEG5000 resulted in a PEG coating surface density of 1.3–2.1, 0.5–0.7, and 1.5–2.0 molecules/nm^2, respectively. They demonstrated that the mixture of two PEG with different chain lengths had no significant effects on the surface coating. In a different study, Sugiyama and Sadzuka found that FALT was not only a function of PEG chain length, but also a function of the type of anchor linking the PEG chain to the surface of the vesicles (37). In their study, they reported that the mixing of 1-monomethoxypolyethyleneglycol-2,3-distearoylglycerol and PEG_{2000} cholesterol (PEG-CHO) in liposome surface modification showed varied FALT results which depends on the anchor type, with the PEG-CHO having a higher FALT value when used alone than in various combination ratios. In our present study, we could infer that

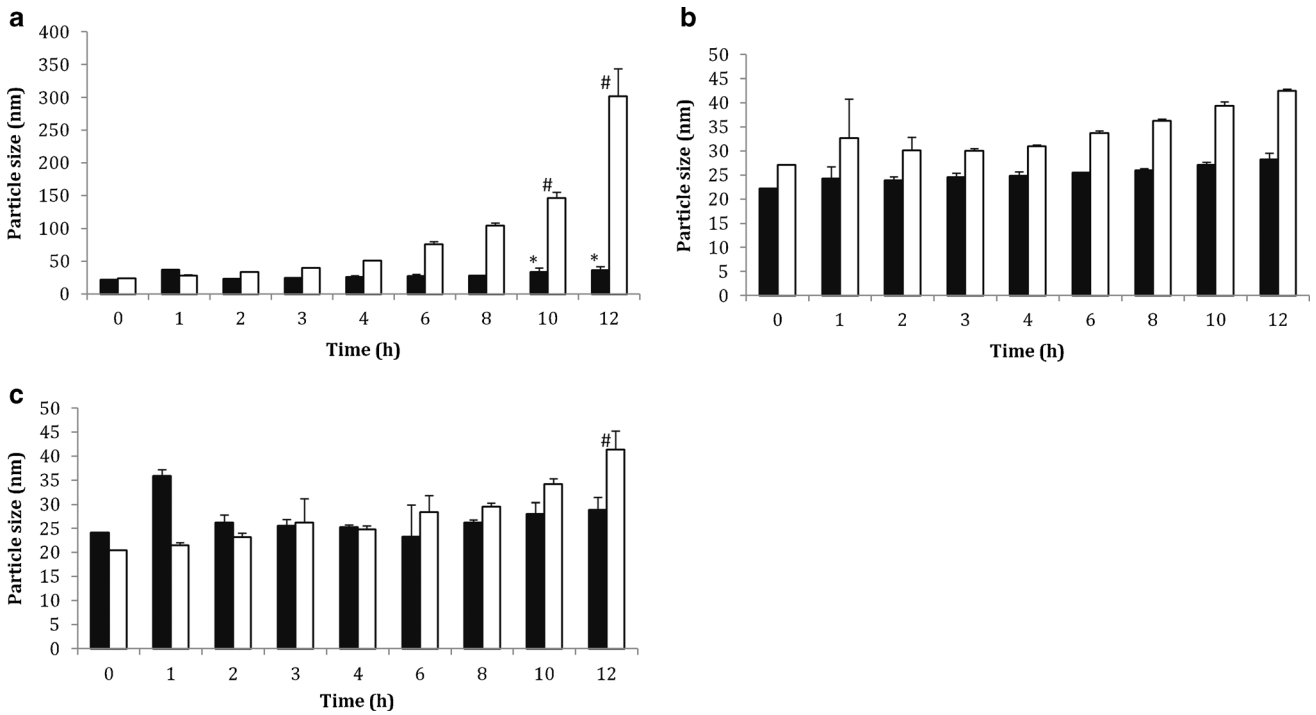

Fig. 5. Stability of breviscapine SLNs in deionized water (*black square*) and PBS 5.8 (*white square*) at 37°C for 12 h: **a** Bre-GMSLN-PS, **b** Bre-GBSLN-PS, and **c** Bre-GBSLN-PS-DSPE. Data are presented as the mean particle size of three separate measurements. *Error bars* represent SD. $^{*}P<0.05$, $^{\#}P<0.001$ *versus* particles size at 0 h

the slightly higher FALT result obtained when PEG-40 stearate was used alone in surface modification was due to the single stearate anchor unit of PEG-40 stearate which was easier to incorporate onto the surface of the SLNs than the double alkyl anchors of the DSPE-PEG_{2000} which would apparently need more space due to the steric hindrance, resulting in lower effective surface binding. The incorporation of the DSPE-PEG_{2000} after the formation of a monolayer of PEG-40 stearate–Solutol HS15 at the surface of the lipid nanoparticles may also have led to the desorption of PEG-40 stearate and Solutol HS15 at a rate which resulted in a less ordered PEG mesh at the surface of the lipid nanoparticles.

Also, for the same reasons, the grafting surface density of PEG in the Bre-GBSLN-PS of 0.013 ± 0.005 molecules/nm^2

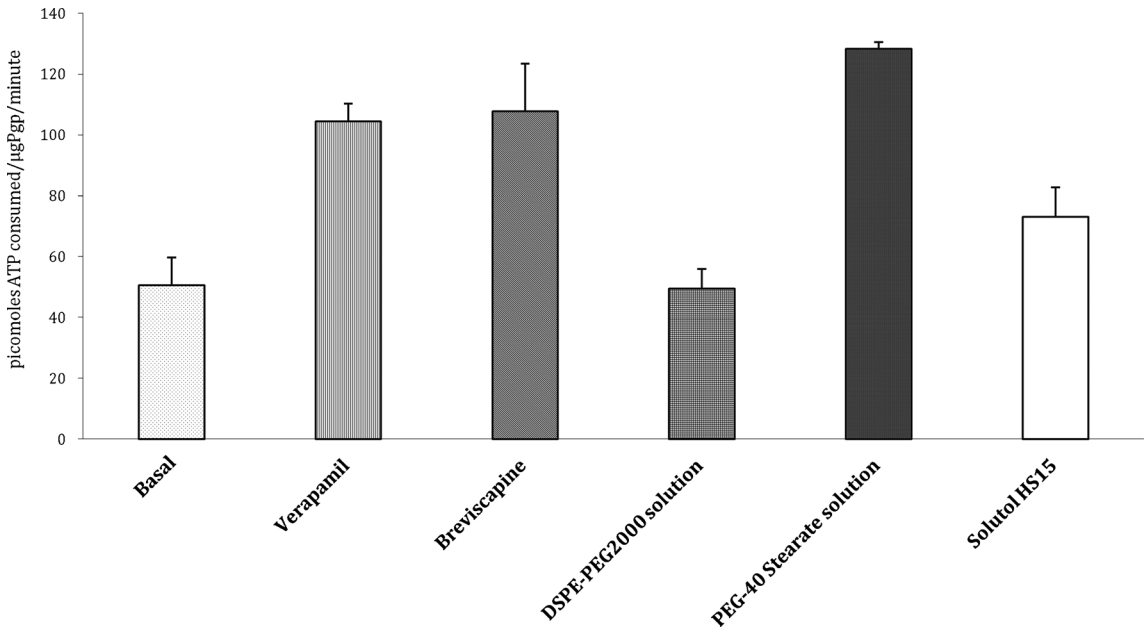

Fig. 6. P-glycoprotein ATPase activity of breviscapine and surfactants used in formulating mixed PEG-modified SLNs. Verapamil was used as a positive control. *Each bar* represents mean value, *error bars* represent SD ($n=3$)

Table II. Fixed Aqueous Layer Thickness, Incorporated Ratio of PEG, Average PEG Surface Density, and Distance Between Two Neighboring PEG Chains of Bre-GBSLN-PS and Bre-GBSLN-PS-DSPE

Formulations	FALT (nm)	IR (%)	SD_{PEG} (molecules/nm^2)	*D* (nm)
Bre-GBSLN-PS	2.01±0.52	29.20±9.89	0.013±0.005	0.113±0.020
Bre-GBSLN-PS-DSPE	1.94±0.13	29.83±3.63	0.012±0.001	0.125±0.004

Each data point represents mean ± SD (n=3)
FALT fixed aqueous layer thickness, *IR* incorporated ratio of PEG, SD_{PEG} average PEG surface density, *D* distance

was not significantly different (p>0.05) from the grafting density of 0.012±0.001 molecules/nm^2 for the Bre-GBSLN-PS-DSPE, but was slightly higher. Therefore, the conformation of PEG chains in the Bre-GBSLN-PS was closely packed with a shorter distance apart (*D*) than the Bre-GBSLN-PS-DSPE. Considering these results and various previous reports on the effects of mixed PEG modification of nano-vesicles, we suggest that a single PEG modification with a PEG molecule of an appropriate chain length could give sufficient stealth properties to the modified nanoparticles as much as a binary mixed PEG modification. However, more investigations are needed to be done to understand the different effects of PEG surface modification of nanoparticle, since the anchor type and not only the PEG molecular weights have effects on the incorporation rates of the PEG chains and consequently on FALT and PEG surface density.

Pharmacokinetics in Plasma

Plasma pharmacokinetic evaluation of the formulated breviscapine SLNs and breviscapine commercial injection were performed in adult male Sprague Dawley rats, and the results were compared to determine the potential of the SLNs to improve brain uptake of breviscapine. The plasma pharmacokinetic profiles of the breviscapine formulations are shown in Fig. 7. The SLN formulations of breviscapine significantly increased the plasma concentrations of scutellarin in comparison with the commercial breviscapine injection (p<0.05). Expectedly, the initial plasma concentration of scutellarin from the commercial breviscapine injection was significantly reduced due to its short half-life and fast elimination from circulation. The SLN formulations extended the circulation time of scutellarin for the first 1 h, after which the plasma concentration decreased as a result of the tissue distribution. The plasma AUCs of scutellarin from breviscapine injection, Bre-GBSLN-PS, and Bre-GBSLN-PS-DSPE were found to be 16.46±4.14, 56.39±8.84, and 31.39±8.82 μg h/mL, respectively (Table III). The plasma AUC was significantly increased by the SLN formulations in comparison with the commercial injection (p<0.05). Modifications of the surface of SLNs with hydrophilic PEG chains have been reported to improve the biological half-life of drugs and increase their circulation time while encapsulated in the SLNs (13). Bre-GBSLN-PS also showed a statistically significant increase in the plasma AUC in comparison with Bre-GBSLN-PS-DSPE (p<0.05). The rapid decrease in the scutellarin concentrations in plasma with the Bre-GBSLN-PS-DSPE after 1 h showed that the drug was increasingly distributed to the other tissues.

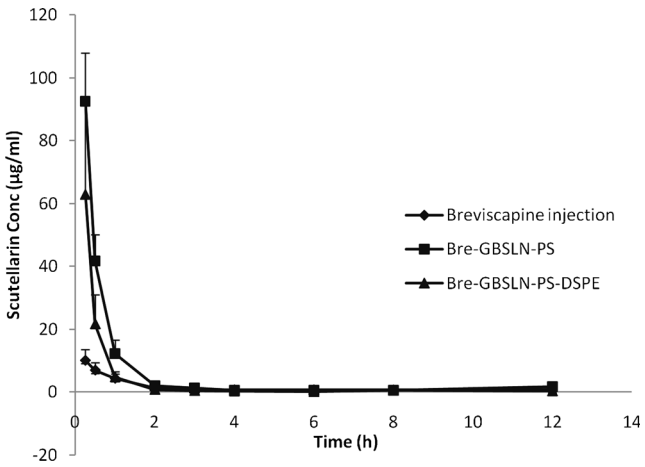

Fig. 7. Plasma scutellarin concentration–time curves after IV administration of 8 mg/kg breviscapine equivalent of commercial breviscapine injection, Bre-GBSLN-PS, and Bre-GBSLN-PS-DSPE through the lateral tail vein. Each *data point* represents mean value, *error bars* represent SD (n=6)

Pharmacokinetics in Brain

The *in vitro* and *in vivo* recoveries for the microdialysis probes were 0.36±0.14 and 0.25±0.07, respectively (Table IV), as determined by the retrodialysis-by-drug method. This showed no significant difference (p>0.05) in relative loss of scutellarin from the perfusate across the probes into the surrounding environment during both *in vitro* and *in vivo* recovery evaluation. For a better quantification of the amount of drug in the brain ECF, the brain concentrations of scutellarin determined in each animal during the microdialysis studies were corrected based on the *in vivo* recovery for each probe. The brain ECF concentration–time curves and brain pharmacokinetic parameters for scutellarin after IV administration of a commercial breviscapine injection, Bre-GBSLN-PS, and Bre-GBSLN-PS-DSPE formulations are showed in Fig. 8 and Table III, respectively. From the results of the AUC in the brain ECF, breviscapine injection, Bre-GBSLN-PS, and Bre-GBSLN-PS-DSPE showed AUCs of 0.11±0.02, 1.59±0.39, and 1.42±0.58 μg h/mL, respectively. The brain-to-plasma AUC ratios ($AUC_{brain\ ECF}/AUC_{plasma}$) also increased with the SLNs in comparison with that of the commercial breviscapine injection. The $AUC_{brain\ ECF}/AUC_{plasma}$ for breviscapine injection, Bre-GBSLN-PS, and Bre-GBSLN-PS-

Table III. Plasma and Brain ECF Pharmacokinetics of Breviscapine After IV Administration of 8 mg/kg Breviscapine Equivalent of Injection Breviscapine, Bre-GBSLN-PS, and Bre-GBSLN-PS-DSPE Through the Lateral Tail Vein

Formulations	$t_{1/2\ Plasma}$ (h)	CL_P (L/h)	$K_{e\ Plasma}$ (h^{-1})	$AUC_{0-12\ h\ Plasma}$ (μg h/mL)	$AUC_{0-12\ h\ brain\ ECF}$ (μg h/mL)	$AUC_{brain\ ECF}/AUC_{plasma}$ (%)	$t_{1/2\ brain\ ECF}$ (h)	$K_{e\ Brain\ ECF}$ (h^{-1})	$MRT_{Brain\ ECF}$ (h)
Breviscapine injection	2.26±1.54	0.51±0.12	0.39±0.16	16.46±4.14	0.11±0.02	0.66	2.19±0.68	0.34±0.13	3.16±0.98
Bre-GBSLN-PS	3.21±1.13	0.15±0.02	0.24±0.07	56.39±8.84***	1.59±0.39***	2.82	4.73±2.02**	0.13±0.04	7.86±2.13*
Bre-GBSLN-PS-DSPE	2.50±0.10	0.27±0.07	0.32±0.13	31.39±8.82*	1.42±0.58**	4.51	3.95±3.67	0.31±0.24	5.70±5.30

Each data point represents mean ± SD, $n=3$ for brain ECF and $n=6$ for plasma pharmacokinetic parameters
*$P<0.05$, **$P<0.01$, ***$P<0.001$ *versus* injection breviscapine

DSPE were found to be 0.66%, 2.82%, and 4.51%, respectively. The $AUC_{brain\ ECF}/AUC_{plasma}$ ratios showed that Bre-GBSLN-PS-DSPE had more brain permeation than the other formulations. This demonstrates that the surface modification of the SLNs with a binary combination of PEG derivatives could increase its brain permeation by a synergistic effect. It was observed that Bre-GBSLN-PS-DSPE had a shorter time ($T_{max}=0.42\pm0.14$ h) to get to maximum concentration ($C_{max}=655.16\pm320.74$ ng/mL) when compared with Bre-GBSLN-PS which took a longer time of 1.17±0.76 h to reach a maximum concentration of 385.24±214.13 ng/mL. However, the single PEG-modified Bre-GBSLN-PS had a significantly longer mean residence time (MRT) in the brain ECF when compared with the breviscapine injection ($p<0.05$) and a higher but not significant ($p>0.05$) MRT when compared with the mixed PEG-modified Bre-GBSLN-PS-DSPE. The additional grafting of DSPE-PEG_{2000} on the surface of the SLNs could have augmented the inhibiting action of PEG-40 stearate on the P-gp efflux pumps leading to a more rapid elimination of breviscapine loaded in the Bre-GBSLN-PS-DSPE from the plasma and increased distribution across tissues where P-gps are overexpressed including the brain. We therefore suggest that the uptake of the breviscapine-loaded SLNs across the BBB was facilitated by the synergistic inhibitory action of PEG derivatives used as the surface modifier for the SLNs on the P-gp efflux pumps. In a previous study to determine the ability of different excipients to inhibit P-gp efflux pumps, Wang *et al.* (14) demonstrated that among the excipients tested, PEG stearates with a moderate PEG length (20 to 50) consistently showed better inhibition of P-gp activity than other PEG derivatives investigated. They also found in their studies that nonionic PEG-poly(propylene oxide) copolymers and PEG of any length did not inhibit P-gp at the concentrations tested. However, the mechanism of inhibition of P-gp efflux pumps by PEG derivatives is not yet fully elucidated (15). Multiple mechanisms might be responsible for the inhibition of P-pg activity by surfactants. Cremophor EL and Tween 80 had been shown to inhibit P-gp activity by specifically binding to its hydrophobic domain and subsequently changing the conformation and reducing the function of the P-gp efflux pumps (38). In this present study, the result obtained from the P-gp ATPase activity showed that PEG-40 stearates could have directly interacted with the substrate-activated P-gp efflux pumps and either competes with the substrate to saturate the P-gp efflux pump receptors for the drug or depletes the available ATP and then inhibits P-gp-mediated efflux. Also, the slight decrease in the P-gp ATPase activity observed for DSPE-PEG indicates that it could act as an inhibitor at the P-gp efflux pumps. The combination of DSPE-PEG and PEG-40 stearate as surface modifications could synergistically inhibit the efflux of breviscapine by the P-gp efflux pumps just as the prolonged circulation time of the SLNs also enhances their penetration of the endothelial membrane either by transcytosis or endocytosis into the brain ECF.

Table IV. Comparison of Microdialysis Probe Recovery Measured *In Vitro* and *In Vivo* by the Retrodialysis Method for the Cerebral Microdialysis Studies

Method	Probe	Recovery	
		In vitro	*In vivo*
Retrodialysis	A	0.27	0.31
	B	0.52	0.26
	C	0.27	0.18
	Mean	0.36	0.25
	SD	0.14	0.07
	CV (%)	40.62	25.94

SD standard deviation, *CV* coefficient of variation

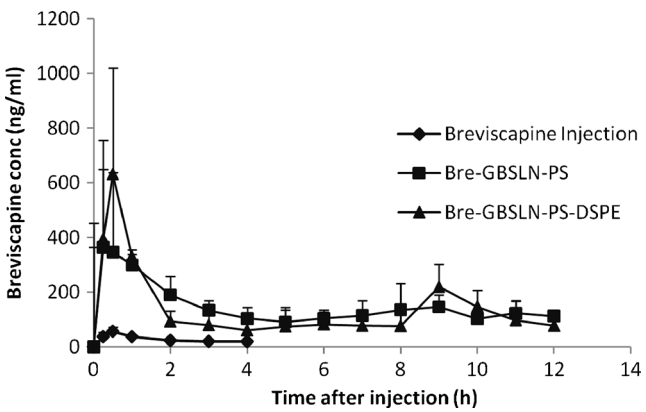

Fig. 8. Brain ECF scutellarin concentration–time curves after IV administration of 8 mg/kg breviscapine equivalent of commercial breviscapine injection, Bre-GBSLN-PS, and Bre-GBSLN-PS-DSPE through the lateral tail vein. Each *data point* represents mean value, *error bars* represent SD ($n=3$)

CONCLUSION

In summary, the formulation of PEG-coated breviscapine-loaded solid lipid nanoparticles was successfully carried out using warm o/w microemulsion precursor approach. Our formulations, Bre-GBSLN-PS and Bre-GBSLN-PS-DSPE, augmented the plasma half-life and increased mean retention time of breviscapine in rats' brain, thereby reducing the necessity of multiple breviscapine injections. On the other hand, we showed that the coating of the optimized SLNs with a binary combination of PEG-40 stearate and DSPE-PEG_{2000} increased brain uptake more than coating with PEG-40 stearate alone as indicated by the brain-to-plasma AUC ratios. Thus, the use of appropriate PEG derivatives in surface modification of SLNs is a promising approach in delivering drug molecules into the brain since it can both effectively improve *in vivo* biostability of the SLNs and passively target biological mechanisms such as the P-gp efflux inhibition. However, our approach needs more *in vivo* studies to understand the mechanism by which the nanoparticles are taken up by the brain endothelial cells.

ACKNOWLEDGMENTS

This study was financially supported by the National Natural Science Foundation of China (81001645), Program for New Century Excellent Talents in University (NCET-12-1068), Tianjin Natural Science Foundation (12JCYBJC18700), and the National Key Technology Research and Development Program of China (2012ZX09304007).

REFERENCES

1. Wang M, Xie C, Cai RL, Li XH, Luo XZ, Qi Y. Studies on antioxidant activities of breviscapine in the cell-free system. Am J Chinese Med. 2008;36(6):1199–207.
2. Cuzzocrea S, Riley DP, Caputi AP, Salvemini D. Antioxidant therapy: a new pharmacological approach in shock, inflammation, and ischemia/reperfusion injury. Pharmacol Rev. 2001;53(1):135–59.
3. Cao W, Liu W, Wu T, Zhong D, Liu G. Dengzhanhua preparations for acute cerebral infarction. Cochrane Database Syst Rev. 2008;4, CD005568. doi:10.1002/14651858.CD005568.pub2.
4. Qian L, Shen M, Tang H, Tang Y, Zhang L, Fu Y, *et al*. Synthesis and protective effect of scutellarein on focal cerebral ischemia/reperfusion in rats. Molecules. 2012;17(9):10667–74. doi:10.3390/molecules170910667.
5. Lv W, Guo J, Li J, Huang L, Ping Q. Distribution of liposomal breviscapine in brain following intravenous injection in rats. Int J Pharm. 2005;306(1–2):99–106. doi:10.1016/j.ijpharm.2005.09.012.
6. Sun H, Dai H, Shaik N, Elmquist WF. Drug efflux transporters in the CNS. Adv Drug Deliv Rev. 2003;55(1):83–105.
7. De Boer AG, Breimer DD. The blood–brain barrier: clinical implications for drug delivery to the brain. J R Coll Physicians Lond. 1994;28(6):502–6.
8. Schinkel AH. P-glycoprotein, a gatekeeper in the blood–brain barrier. Adv Drug Deliv Rev. 1999;36(2–3):179–94.
9. Liu M, Li H, Luo G, Liu Q, Wang Y. Pharmacokinetics and biodistribution of surface modification polymeric nanoparticles. Arch Pharm Res. 2008;31(4):547–54. doi:10.1007/s12272-001-1191-8.
10. She Z-Y, Ke X, Ping Q, Xu B-H, Chen B. Preparation of breviscapine nanosuspension and its pharmacokinetic behavior in rats. Chin J Nat Med. 2007;5(1):50–5.
11. Dingler A, Runge S, Muller RH. SLN (solid lipid nanoparticles) as drug carrier for an IV administration of poorly water soluble drugs. Eur J Pharm Sci. 1996;4(1001):132. doi:10.1016/s0928-0987(97)86382-8.
12. Silva GA. Nanotechnology approaches to crossing the blood–brain barrier and drug delivery to the CNS. BMC Neurosci. 2008;9 Suppl 3:S4. doi:10.1186/1471-2202-9-S3-S4.
13. Madan J, Pandey RS, Jain V, Katare OP, Chandra R, Katyal A. Poly (ethylene)-glycol conjugated solid lipid nanoparticles of noscapine improve biological half-life, brain delivery and efficacy in glioblastoma cells. Nanomedicine. 2013;9(4):492–503. doi:10.1016/j.nano.2012.10.003.
14. Wang SW, Monagle J, McNulty C, Putnam D, Chen H. Determination of P-glycoprotein inhibition by excipients and their combinations using an integrated high-throughput process. J Pharm Sci. 2004;93(11):2755–67. doi:10.1002/jps.20183.
15. Zhu S, Huang R, Hong M, Jiang Y, Hu Z, Liu C, *et al*. Effects of polyoxyethylene (40) stearate on the activity of P-glycoprotein and cytochrome P450. Eur J Pharm Sci. 2009;37(5):573–80. doi:10.1016/j.ejps.2009.05.001.
16. Sawchuk RJ, Elmquist WF. Microdialysis in the study of drug transporters in the CNS. Adv Drug Deliv Rev. 2000;45(2–3):295–307.
17. Subedi RK, Kang KW, Choi HK. Preparation and characterization of solid lipid nanoparticles loaded with doxorubicin. Eur J Pharm Sci. 2009;37(3–4):508–13. doi:10.1016/j.ejps.2009.04.008.
18. Oyewumi MO, Mumper RJ. Gadolinium-loaded nanoparticles engineered from microemulsion templates. Drug Dev Ind Pharm. 2002;28(3):317–28. doi:10.1081/ddc-120002847.
19. Yue PF, Lu XY, Zhang ZZ, Yuan HL, Zhu WF, Zheng Q, *et al*. The study on the entrapment efficiency and in vitro release of puerarin submicron emulsion. AAPS PharmSciTech. 2009;10(2):376–83. doi:10.1208/s12249-009-9216-3.
20. Shimada K, Miyagishima A, Sadzuka Y, Nozawa Y, Mochizuki Y, Ohshima H, *et al*. Determination of the thickness of the fixed aqueous layer around polyethyleneglycol-coated liposomes. J Drug Target. 1995;3(4):283–9. doi:10.3109/10611869509015957.
21. Peracchia MT, Vauthier C, Passirani C, Couvreur P, Labarre D. Complement consumption by poly(ethylene glycol) in different conformations chemically coupled to poly(isobutyl 2-cyanoacrylate) nanoparticles. Life Sci. 1997;61(7):749–61.
22. Litman T, Zeuthen T, Skovsgaard T, Stein WD. Structure-activity relationships of P-glycoprotein interacting drugs: kinetic characterization of their effects on ATPase activity. Biochim Biophys Acta. 1997;1361(2):159–68.
23. Lonnroth P, Jansson PA, Smith U. A microdialysis method allowing characterization of intercellular water space in humans. Am J Physiol. 1987;253(2 Pt 1):E228–31.
24. Wang Y, Wong SL, Sawchuk RJ. Microdialysis calibration using retrodialysis and zero-net flux: application to a study of the distribution of zidovudine to rabbit cerebrospinal fluid and thalamus. Pharm Res. 1993;10(10):1411–9.
25. Zhong D, Yang B, Chen X, Li K, Xu J. Determination of scutellarin in rat plasma by high-performance liquid chromatography with ultraviolet detection. J Chromatogr B Analyt Technol Biomed Life Sci. 2003;796(2):439–44.
26. Burra M, Jukanti R, Janga KY, Sunkavalli S, Velpula A, Ampati S, *et al*. Enhanced intestinal absorption and bioavailability of raloxifene hydrochloride via lyophilized solid lipid nanoparticles. Adv Powder Technol. 2013;24(1):393–402. doi:10.1016/j.apt.2012.09.002.
27. Li S, Ji Z, Zou M, Nie X, Shi Y, Cheng G. Preparation, characterization, pharmacokinetics and tissue distribution of solid lipid nanoparticles loaded with tetrandrine. AAPS PharmSciTech. 2011;12(3):1011–8. doi:10.1208/s12249-011-9665-3.
28. Juillerat-Jeanneret L. The targeted delivery of cancer drugs across the blood–brain barrier: chemical modifications of drugs or drug-nanoparticles? Drug Discov Today. 2008;13(23–24):1099–106.
29. Muller RH, Mader K, Gohla S. Solid lipid nanoparticles (SLN) for controlled drug delivery—a review of the state of the art. Eur J Pharm Biopharm. 2000;50(1):161–77.
30. Peltonen L, Aitta J, Hyvonen S, Karjalainen M, Hirvonen J. Improved entrapment efficiency of hydrophilic drug substance

during nanoprecipitation of poly(l)lactide nanoparticles. AAPS PharmSciTech. 2004;5(1):E16. doi:10.1208/pt050116.
31. Cao F, Guo JX, Ping QN, Liao ZG. Prodrugs of scutellarin: ethyl, benzyl and N,N-diethylglycolamide ester synthesis, physicochemical properties, intestinal metabolism and oral bioavailability in the rats. Eur J Pharm Sci. 2006;29(5):385–93. doi:10.1016/j.ejps.2006.07.007.
32. Tsai MJ, Huang YB, Wu PC, Fu YS, Kao YR, Fang JY, *et al*. Oral apomorphine delivery from solid lipid nanoparticles with different monostearate emulsifiers: pharmacokinetic and behavioral evaluations. J Pharm Sci. 2011;100(2):547–57. doi:10.1002/jps.22285.
33. Souto EB, Muller RH. Investigation of the factors influencing the incorporation of clotrimazole in SLN and NLC prepared by hot high-pressure homogenization. J Microencapsul. 2006;23(4):377–88. doi:10.1080/02652040500435295.
34. Dong X, Mattingly CA, Tseng MT, Cho MJ, Liu Y, Adams VR, *et al*. Doxorubicin and paclitaxel-loaded lipid-based nanoparticles overcome multidrug resistance by inhibiting P-glycoprotein and depleting ATP. Cancer Res. 2009;69(9):3918–26. doi:10.1158/0008-5472.can-08-2747.
35. Kopecka J, Salzano G, Campia I, Lusa S, Ghigo D, De Rosa G, *et al*. Insights in the chemical components of liposomes responsible for P-glycoprotein inhibition. Nanomedicine. 2013. doi:10.1016/j.nano.2013.06.013.
36. Cauda V, Argyo C, Bein T. Impact of different PEGylation patterns on the long-term bio-stability of colloidal mesoporous silica nanoparticles. J Mater Chem. 2010;20(39):8693–9.
37. Sugiyama I, Sadzuka Y. Characterization of novel mixed polyethyleneglycol modified liposomes. Biol Pharm Bull. 2007;30(1):208–11.
38. Shono Y, Nishihara H, Matsuda Y, Furukawa S, Okada N, Fujita T, *et al*. Modulation of intestinal P-glycoprotein function by cremophor EL and other surfactants by an in vitro diffusion chamber method using the isolated rat intestinal membranes. J Pharm Sci. 2004;93(4):877–85. doi:10.1002/jps.20017.